Received: 27 February 2018 | Revised: 24 May 2018 | Accepted: 6 August 2018

DOI: 10.1002/suco.201800058

WILEY fib

TECHNICAL PAPER

Corrosion behavior and optimization of air-entrained reinforced concrete, incorporating microsilica

Anis Ghanei[1] | Hamid Eskandari-Naddaf[1] | Ali Davoodi[2]

[1]Department of Civil Engineering, Hakim Sabzevari University, Sabzevar, Iran

[2]Materials and Metallurgical Engineering Department, Faculty of Engineering, Ferdowsi University of Mashhad, Mashhad, Iran

Correspondence
Hamid Eskandari-Naddaf, Department of Civil Engineering, Hakim Sabzevari University, Sabzevar, Iran.
Email: hamidiisc@yahoo.com

Nowadays, corrosion evaluation of steel embedded in reinforced concrete (RC) plays an important role in repair, protection and maintenance of RC structures. Air-entraining agent (AEA) and microsilica (MS) are among the most important admixtures, which affect the corrosion rate (CR) of RC. Specifically, 12 mix designs incorporating different contents of AEA (ie, 0, 0.7, 1.4, 2.1, 2.9, and 3.6% by weight), half with 10% MS, were constructed. The corrosion behavior of RC specimens after exposure to 3.5% NaCl environment was investigated using half-cell potential (HCP) and electrical resistance (ER) as conventional tests and Tafel polarization as a more powerful corrosion test. Moreover, an optimization process was conducted on the mix design parameters using Taguchi and Factorial methods to analyze the effective factors and sensitivity of CR to each factor. The results of Tafel test indicate that they are noticeably more reliable and reasonable as compared to HCP and ER tests. Moreover, the results show that incorporating a low content of AEA (up to 0.7%) effectively improves the corrosion behavior of RC specimens, while the mix design containing 0.7% AEA together with 10% MS is the optimal design in terms of a decreased CR. The results also show that Factorial is a more applicable method in the field of corrosion evaluation of RC, due to the yield of more accurate findings as compared to Taguchi.

KEYWORDS

air-entraining agent, corrosion, microsilica, optimization, Tafel polarization

1 | INTRODUCTION

Penetration of chloride ions into steel surfaces causes corrosion and thus, reduces lifetime of reinforced concrete (RC) structures. Therefore, research on reduction of the concrete permeability which can lead to a reduced corrosion, has been of great interest.[1] One of the factors that can increase RC life time against freeze-thawing cycles[2,3] and permeability[4,5] is air-entraining agent (AEA). The accurate content of AEA that can effectively improve or negatively affect the permeability properties of RC has not yet been determined. In this way, researchers have reported both positive[6,7] and negative[8] effects of AEA on permeability and corrosion properties of RC. Due to this, it can be mentioned that the reason for lack of clarity in the effects of AEA on corrosion of RC is the method of evaluating the corrosion behavior of RC from the results of permeability test at which some significant errors may be included, or using half-cell potential (HCP)[9] and electrical resistivity (ER)[10] tests, which are among the conventional methods of determining permeability[11] and corrosion of concrete.[12] The ER value generally states the corrosion progress in RC as a dependent parameter on the hardened cement paste,[11] while the HCP value expresses the probability of the corrosion phenomenon.[13,14] Therefore, it is not possible to determine the positive or negative effect of AEA on corrosion behavior of RC using these two methods, due to their insufficient accuracy.

Microsilica (MS) is another factor, whose effects can be considered in this field. It is well established that MS can be typically used to reduce the permeability of chloride in

concrete.[15] In this regard, researchers have conducted valuable studies on the use of MS, to reduce permeability[16] and corrosion,[17–19] and to increase strength,[20,21] durability[22] and electrical resistance[23,24] of RC. They have also provided optimal values for each factor in order to improve the desired properties of RC. For instance, studies were carried out on concrete containing MS to investigate the corrosion properties of RC by electrochemical experiments and the results indicated that the optimal amount of MS is 10% by weight,[7,9] and the higher amounts may increase the corrosion rate (CR).[7]

Considering the above mentioned facts, it was found out that similar to MS with a reported optimal amount in the case of improving the corrosion behavior of RC, there was a significant need to indicate the optimal amount of AEA. In this regard, the combined effect of MS and AEA on permeability of concrete was evaluated in the study of Choi et al.[5] Their results indicated that increase in the MS amount from 0 to 9% leads to a decreased permeability of 58 to 60%, while addition of this amount of MS in an air-entrianed concrete decreased the permeability from 40 to 60%. Thus, it can be concluded that there is no certain amount reported for AEA alone and also, its combination with MS in order to obtain the lowest permeability in RC. On the other hand, considering that permeability is a corrosion-dependent parameter, investigation of corrosion in such RC structures using powerful methods and accurate determination of the optimal amount of these two additives can be of great interest and significance. Accordingly, in this study, 12 mix designs (6 with only AEA and 6 with combination of AEA and MS) were constructed and exposed to 3.5% NaCl environment. For evaluation of the capability of the conventional methods, the corrosion behavior of RC specimens was first investigated by HCP and electrical resistance (ER). Then, the Tafel polarization technique as a more powerful corrosion test, was conducted on whole specimens. Furthermore, an optimization process was conducted using Taguchi and Factorial methods to obtain the optimal content of AEA and MS and their percentage contribution in terms of the lowest CR. Finally, a comparison study was conducted on the results of applying experimental tests and statistical methods, to specify their effectiveness and distinguish the most efficient methods in the field of corrosion behavior of RC specimens.

2 | EXPERIMENTAL PLAN

2.1 | Materials

In this study, cement type II was Ordinary Portland cement (CEM II 52.5 N),[25–27] fine and coarse aggregate, MS, AEA and super-plasticizer used in mix designs. Tables 1 and 2 respectively, illustrate the chemical and physical properties of the cementitious materials used in the mix designs.

TABLE 2 The physical properties of the Portland cement used[53]

	Blain	Setting time (min)	Setting time (max)	Soundness	Aut.Exp.
Cement	3,083	119	218	Good	0.12
Allowable scale	Min ≥ 2800	Min 45≥	Max ≤360	—	Max ≤0.8

The fine and coarse aggregates used in the mix designs were proposed according to the ASTM C136.[28] Six different contents of AEA (0, 0.7, 1.4, 2.1, 2.9, and 3.6% by weight) were also applied in mix designs conforming to ASTM C260.[29] The specific gravity of 1.01 g/cm^3 and pH of about 7 were also reported for the AEA utilized. Since previous researches concluded that 10% weight of MS replacement can be the optimal amount,[9] this constant content of replacement was applied in half of the mix designs of the current study.

Details of mix designs are shown in Table 3, where a series of 12 cylindrical RC specimens, 10 cm in diameter and 15 cm in height, were constructed. A St37 steel rebar with a diameter of 14 mm and a length of 150 mm was proposed in the middle of each specimen. In order to minimize the crevice corrosion and possible localized attacks in the specimens, their concrete–steel–atmosphere interfaces were insulated with epoxy resin; the lengths of steel rebar outside the specimen was 50 mm, while the length in contact with concrete was 80 mm (Figure 1).

After 24 hr, the specimens were demolded and wet-cured for 28 days at the curing tank. Finally, the RC specimens were exposed to 3.5% NaCl solution for 2 weeks accompanied by 2 weeks in dry condition.

2.2 | Methods

Figure 2 is the schematic of HCP measurement in the 3.5% NaCl solution (artificial seawater). This process was done to simulate marine environments for the half-cell measurement according to ASTM C876-09[30] and a reference electrode was used for the copper/copper sulfate electrode.

Figure 3 gives the schematic view of the ER test which was conducted on specimens according to ASTM C1760[31] and based on Ohm's Law.[32] The test was carried out at 20°C and ER values were measured by the two-electrode method using external steel plates and a hand-held resistance meter with a frequency of 1 kHz. The calculations of ER of the test specimens were done using Equation (1)

TABLE 1 The chemical compositions of the Portland cement used[51,52]

Ingredient	SiO_2	AL_2O_2	Fe_2O_3	CaO	MgO	K_2O	SO_3	Na_2O	LOI
CEM II 52.5 N	21.54	4.95	3.82	63.24	1.55	0.75	2.43	0.48	1.24

TABLE 3 Details of mix desings applied to produce the test specimens

Mix no.	Water (kg/m^3)	Water/ Cement	Aggregates (kg/m^3)	AEA %	MS (%)	Super-plasticizer (kg/m^3)
A0	278	0.5	1,586	0	—	—
A1	278	0.5	1,586	0.7	—	—
A2	278	0.5	1,586	1.4	—	—
A3	278	0.5	1,586	2.1	—	—
A4	278	0.5	1,586	2.9	—	—
A5	278	0.5	1,586	3.6	—	—
A0M	222	0.4	1,586	0	10	8
A1M	222	0.4	1,586	0.7	10	8
A2M	222	0.4	1,586	1.4	10	8
A3M	222	0.4	1,586	2.1	10	8
A4M	222	0.4	1,586	2.9	10	4
A5M	222	0.4	1,586	3.6	10	2

AEA = air-entraining agent; MS = microsilica.

$$\rho = R\frac{A}{L}, \tag{1}$$

where, ρ is the ER, R is electrical resistance, A is surface area and L is height of the specimen.

The electrical resistance (R) can also be obtained from Equation (2):

$$R = \frac{V}{I}, \tag{2}$$

where, V is potential difference and I is current.

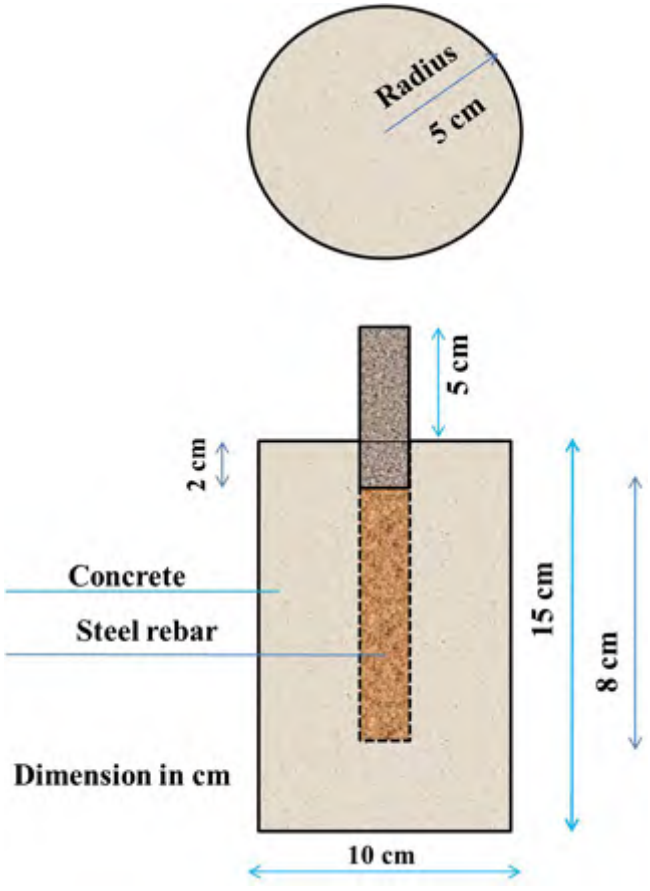

FIGURE 1 Dimension of reinforced concrete specimen

Tafel polarization test was also conducted on specimens by A Gill AC laboratory potentio stat (ACM instrument). The specimens were performed in a 3.5 M NaCl solution. The logarithmic current curves are illustrated by the results of the Tafel test, and the type of analysis is referred to as Tafel slope analysis.[33]

2.3 | Statistical procedures

There are several methods for designing optimal structures,[34] therefore, this paper applied both Taguchi and Factorial methods to highlight the application and compare the effectiveness of their evaluation and optimization processes on parameters affecting the corrosion behavior of RC. It was reported that each of the methods (Taguchi and Factorial methods) has its individual characteristics. The advantages of Taguchi method are reduction of number of experiments, costs and time, and reduction of sensitivity of the system to sources of variation,[35,36] while the advantage of full factorial method is that it produces more accurate results as compared to Taguchi method. However, it is

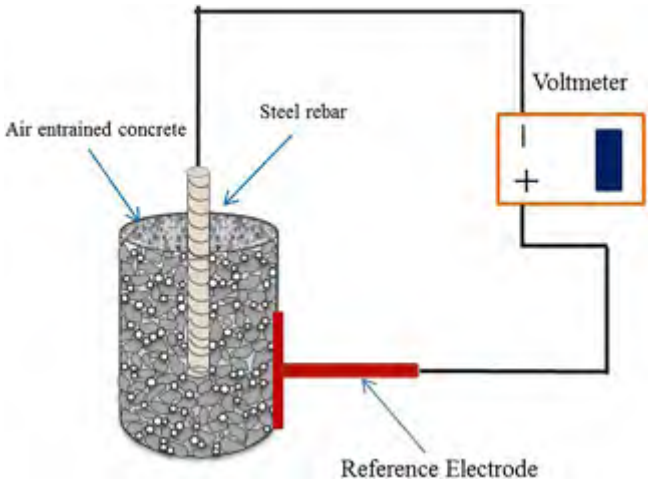

FIGURE 2 Schematic of the half-cell potential measurement setup for air-entrained specimens

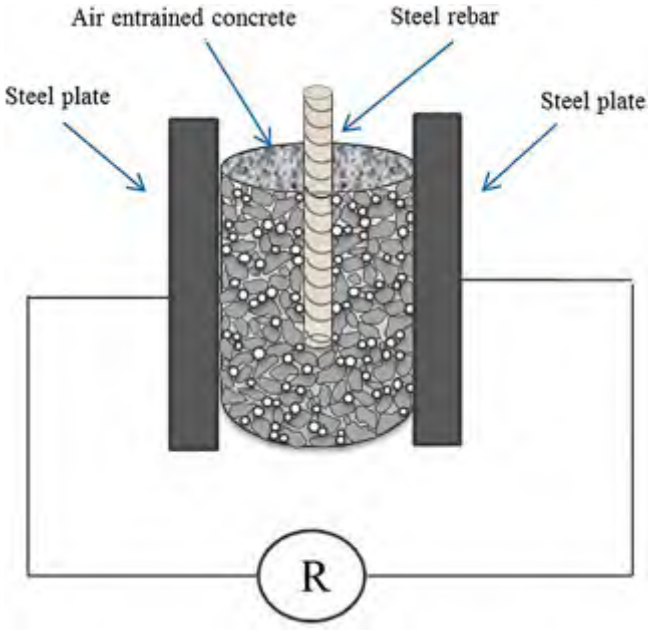

FIGURE 3 Schematic of the electrical resistance measurement setup for air-entrained specimens

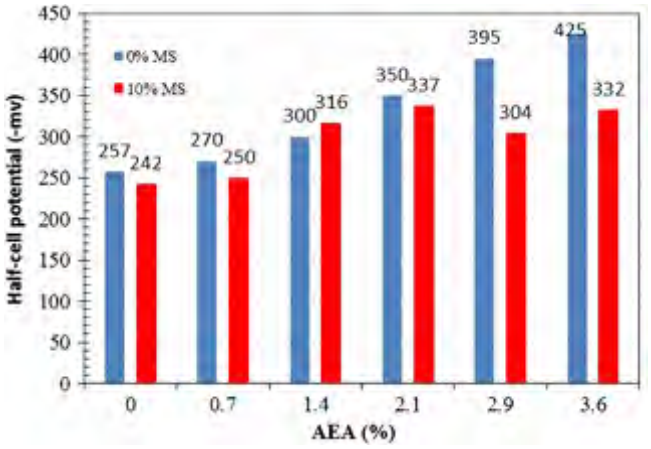

FIGURE 4 Half-cell potential of the air-entrained specimens

difficult to say which method is better. It depends on the experience of the researcher, the time and resources, and how accurate the results are in each case.[37]

In the case of this study, the responses are the values of HCP, ER and CR. Two main factors were also considered in the optimization process, including AEA and MS with six and two levels, respectively, which can be effectively controlled (Table 4). The Minitab software (Version 18, Minitab Inc. State College, PA) was applied to analyze the obtained compositions.

In the Taguchi method, an optimal composition can be determined using the signal-to-noise (S/N) ratios. The term "signal" defines the desirable value and "noise" defines the undesirable value. The S/N ratio is used to calculate the variation and relation of the response to the target value under different noise conditions, so that the sensitivity of the system to the sources of variation decreases, thus resulting in good performance.[20] In this efficient way, the important factors from a large number of potential factors can be detected. Then, the factorial design can be utilized to analyze the interactions among the important factors.[38]

In this paper, ANOVA analysis was carried out to determine statistical significant process parameters and percent contribution of these parameters to the HCP, ER and CR values of RC specimens produced with MS and AEA. ANOVA indicates the contribution of factors and their interactions. ANOVA employs sums of squares which are mathematical abstracts that are used to separate the overall variance in the response to variances due to the processing parameters and measurement errors.[39]

3 | RESULTS AND DISCUSSION

The HCP of RC specimens in 3.5 wt% NaCl solution was measured and the results are shown in Figure 4. Potentials that are lower than −350 mV indicate that the probability of corrosion is more than 90%. For values higher than −200 mV, it can be stated that the probability of corrosion is less than 5%, while the values between −200 and −350 indicate an uncertain corrosion.[40,41] As shown, for air-entrained concrete specimens containing 2.1, 2.9 and 3.6% AEA (A3–A5), the probability of corrosion is more than 90%, while the specimens containing 0 to 1.4% AEA are in uncertain condition. In addition, it can be observed that the absolute HCP values of air-entrained concrete specimens incorporating MS (%) are typically lower than those of air-entrained concrete specimens. This can be attributed to the effect of MS on decrease in the probability of corrosion in such specimens.

The ER measurement of concrete is used as an important method in monitoring the reinforcement of CR. The ER results of all the specimens are presented in Figure 5. The ER of concrete related to the microstructure of the cement paste,[42] is a measure of the permeability of concrete against the entry of corrosive ions like chlorine.[43] Accordingly, Figure 4 shows that 10% cement replacement by MS increases the ER of concrete. This can be due to the role of MS additive in reducing the permeability of cement paste

TABLE 4 The defined factors and their levels

Factor (%)	Level 1	Level 2	Level 3	Level 4	Level 5	Level 6
AEA	3.6	2.9	2.1	1.4	0.7	0
MS	0	10	—	—	—	—

AEA = air-entraining agent; MS = microsilica.

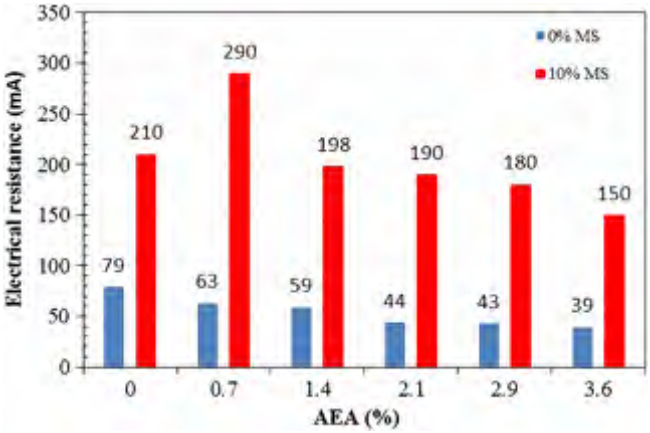

FIGURE 5 Electrical resistance of the air-entrained specimens

when the pores of cement matrix are filled with C-S-H gel produced from pozzolanic activities.[44] This confirms the findings of recent studies,[45,46] which indicated that incorporating MS additive and other cementitious materials such as fly ash and ground granulated blast furnace slag reduces the pores of the cement paste, leading to increase in ER. Furthermore, it is shown in Figure 4 that among the first six specimens (A0–A5), increase in the AEA content decreased the ER of the specimens. However, the results of previous studies have established the positive effects of AEA on decrease in the ER of concrete specimens. In this regard, it was reported that AEA produces discrete, almost spherical bubbles in the cement paste, and no channels were formed for the flow of water and the permeability of the concrete did not increase.[7] On the other hand, the results of ER test on the second six specimens, in which 10% MS was included (A0M–A5M), indicate that the A1M specimen containing 0.7% AEA has the highest ER, which is in contrast with the results of A0–A5 specimens.

Tables 5 and 6 show the results of ANOVA of HCP and ER tests, respectively, for both Taguchi and Factorial methods. It can be observed that the most effective factor on HCP value is AEA (%), while in ER test, MS (%) has more significant effect on response.

Effects of parameters on mean S/N ratio of the (a) HCP and (b) ER tests are illustrated in Figure. 6. As shown, smaller is better type of quality properties was chosen for HCP test as the objective is to minimize the target, while larger is better type was chosen for ER test in order to maximize the target. It was observed that the optimal values of AEA and MS were 0 and 10%, respectively, for HCP test, while the corresponding values for ER test were 0.7 and 10%, respectively. Similar findings are also shown in Figure 7 for both HCP and ER tests.

Comparison of the whole experimental and statistical findings obtained from the HCP and ER tests (Figures 4–7 and Tables 5 and 6) of this study, indicate that these results, in the case of RC specimens, are not in a specific direction and with an acceptable trend. Therefore, it can be concluded that a more powerful method like electrochemical technique is necessary to obtain more reasonable and reliable results. In this way, the Tafel polarization test was conducted on the whole specimens and the results in terms of experimental and statistical analyses are represented in Figures 8–13 and Tables 7 and 8.

As shown in Figure 8, the specimen A5, incorporating the highest content of AEA has the least potential as compared to the other specimens. A gradual decrease of the AEA content increases the potential. This admixture can also increase the current density (i_{corr}) of the specimens, which causes the higher permeability. The obtained results can be confirmed by the findings of a previous study,[8] where high water penetrability was concluded in the case of using high contents of AEA in concrete structures. However, the specimen A1 incorporating 0.7% AEA leads to the highest potential and the lowest i_{corr} among the air-entrained contained specimens. This shows that a low content of AEA can have some beneficial effects on enhancement of the corrosion potential, resulting in a reduced permeability. This can be confirmed by the findings of previous studies,[47,48] which indicate that if there is a high amount of air bubbles in cement paste, the voids will be filled more expressively with hydration products. In fact, incorporating high AEA content causes a greater porosity of the cement paste, leading to the

TABLE 5 ANOVA of HCP test for Taguchi and factorial methods

	Taguchi method			Factorial method			
Source	DF	SS	Contribution (%)	DF	SS	Contribution (%)	Difference (%)
AEA (%)	5	26,798	74.87	5	25,257	70.57	4.3
MS (%)	6	8,990	25.12	6	10,531	29.42	4.3

AEA = air-entraining agent; MS = microsilica.

TABLE 6 ANOVA of ER test for Taguchi and full factorial methods

	Taguchi method			Factorial method			
Source	DF	SS	Contribution (%)	DF	SS	Contribution (%)	Difference (%)
AEA (%)	5	8,274	10.54	5	6,834	8.70	1.84
MS (%)	6	70,209	89.45	6	71,649	91.29	1.84

AEA = air-entraining agent; MS = microsilica.

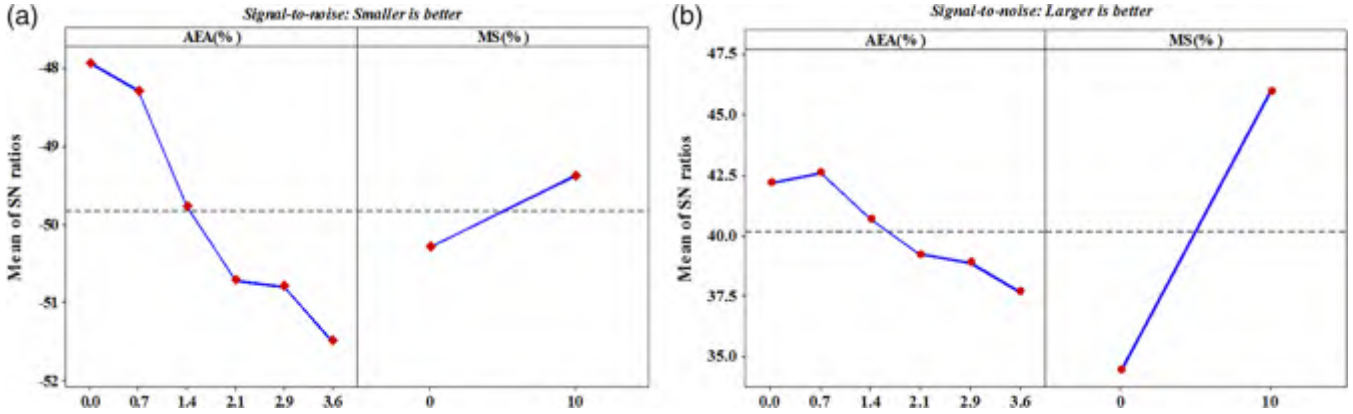

FIGURE 6 Effects of parameters on mean S/N ratio of the (a) half-cell potential and (b) electrical resistance tests

FIGURE 7 The optimization responses obtained from factorial method for half-cell potential and electrical resistance tests

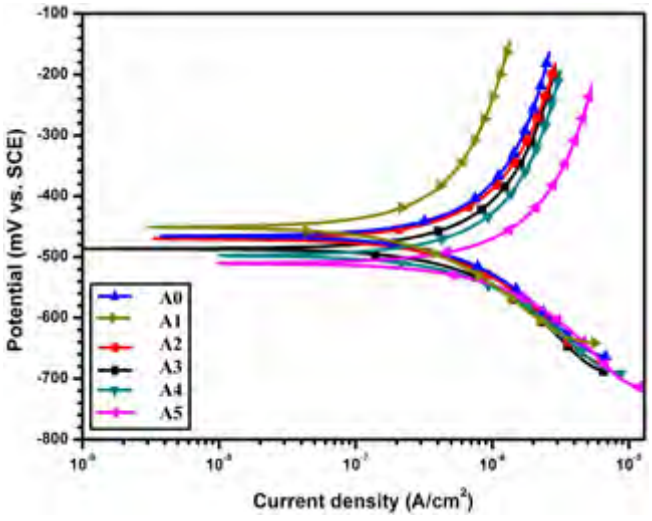

FIGURE 8 Tafel curves of the air-entrained specimens of polarization test. Sample codes (A0–A5) indicate percentage of air-entraining agent as follows: A0 = 0%, A1 = 0.7%, A2 = 1.4%, A3 = 2.1%, A4 = 2.9%, and A5 = 3.6% AEA

presence of capillary channels and micropores in the vicinity of the pores, and the greater ease of water flow between them. Therefore, the CR can be reduced as a result of decrease in oxygen diffusion which helps the H+ ions in concrete to be consumed in the cathodic reaction (Figure 9).

From Figure 10, it can be observed that the potential and i_{corr} of the specimens A0M-A5M are typically enhanced as compared to those of the specimens, A0–A5, which is due to MS existence in the corresponding mix designs.

Contribution of ANOVA of CR test to both Taguchi and Factorial methods are shown in Table 7, indicating the statistical effect of each factor on responses. It can be observed that the most effective factor on CR test is MS due to its higher percent contribution.

The mean values in terms of S/N ratio for both control factors are shown in Figure 11, with the main effects of parameters on the mean responses. As shown, the mean S/N ratio of CR test has higher values, with better results than the other two tests (Figure 6). In addition, it was observed that MS factor is a more important parameter due to its higher S/N value as compared to AEA. Moreover, it can be concluded that the specimen containing 0.7% AEA and 10% MS has the optimal mix design, resulting in the lowest CR value.

The interaction plots of the responses with consideration of the AEA and MS factors are shown in Figure 12. There are considerable interaction effects of factors on response when two lines intersect with each other; in other words, the influence of one factor on the response is altered by the change of level of another factor.[49] It was observed that the interaction plots of both factors are not parallel to each other, indicating that the interaction effects of both factors on responses are so significant.

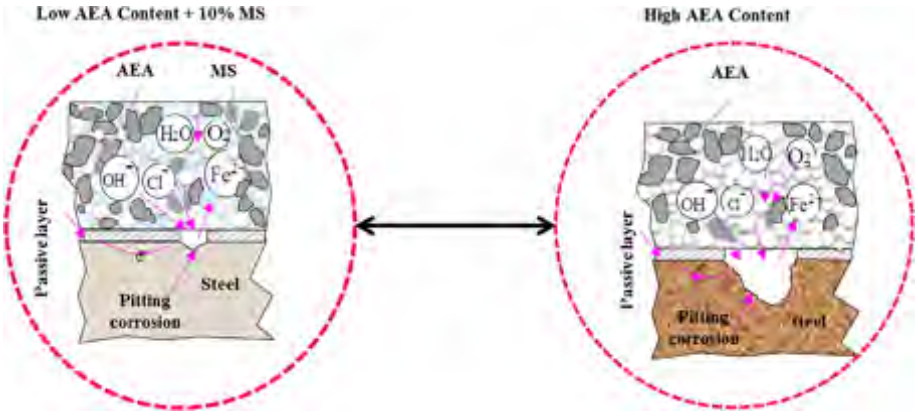

FIGURE 9 Schematic view of electrochemical corrosion of specimens exposed to chloride environment

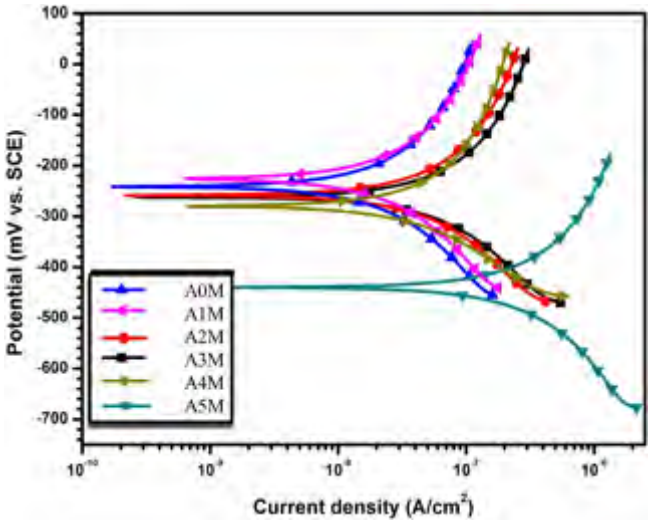

FIGURE 10 Tafel curves of the air-entrained specimens incorporating 10% MS additive of polarization test. Specimen codes (A0M–A5M) indicate the presence of 10% MS and different percentages of AEA: A0M = 0%, A1M = 0.7%, A2M = 1.4%, A3M = 2.1%, A4M = 2.9% and A5M = 3.6%

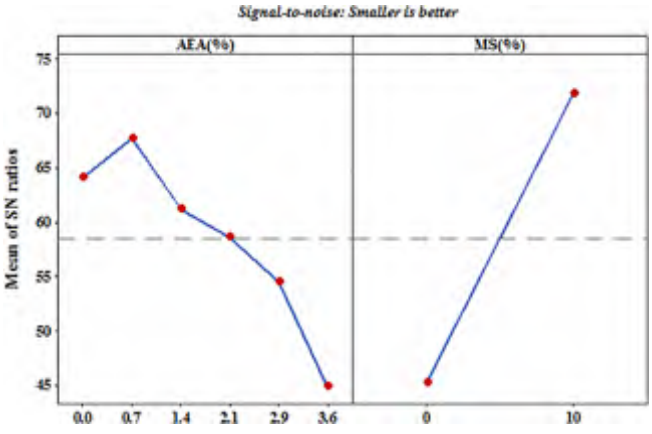

FIGURE 11 Effects of parameters of mean S/N ratio on corrosion rate

Figure 13 shows the optimization values obtained from factorial method for CR test. It was observed that the specimen containing 0.7% AEA and 10% MS is the best mix

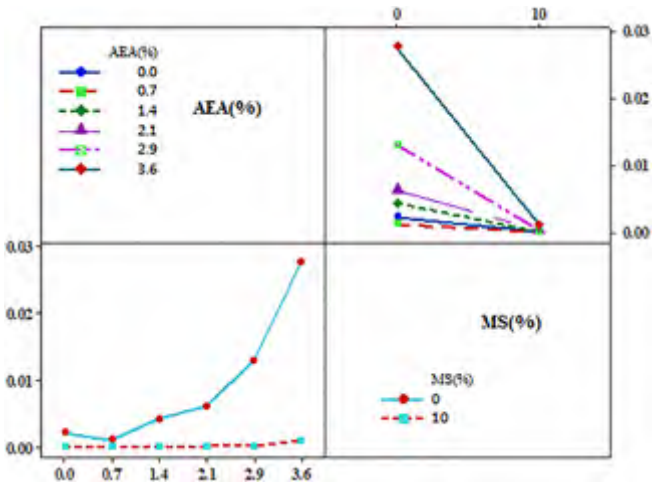

FIGURE 12 Interaction effects of factors on corrosion rate

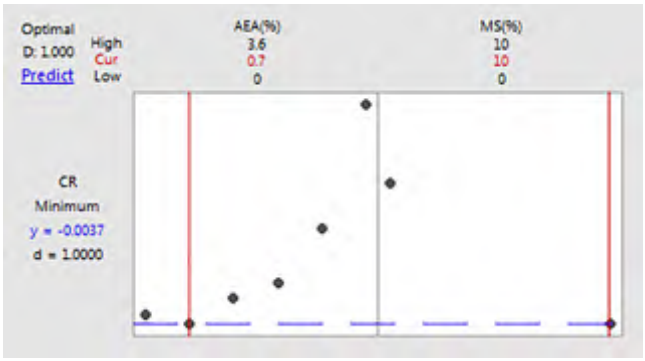

FIGURE 13 The optimization responses obtained from factorial method for corrosion rate test

design, confirming again, the positive effects of combination of MS and a low content of AEA on improvement of concrete characteristics, resulting in decrease in CR.

For comparison of the applicability of Taguchi and Factorial methods in evaluation of factors affecting the corrosion behavior of RC specimens of the current study, an investigation based on R-square values of the analyses for the whole tests was conducted and the results are shown in

TABLE 7 ANOVA of CR test for Taguchi and full factorial methods

	Taguchi design			Factorial method			
Source	**DF**	**SS**	**Contribution (%)**	**DF**	**SS**	**Contribution (%)**	**Difference (%)**
AEA (%)	5	0.0003	42.85	5	0.0003	42.85	0%
MS (%)	6	0.0005	71.42	6	0.0004	57.14	14.28

AEA = air-entraining agent; MS = microsilica; DF = Degree of freedom; SS = Sums of squares.

TABLE 8 R^2 (%) for different tests according to Taguchi and factorial methods

	R^2 (%)	
Test	**Factorial method**	**Taguchi method**
HCP	87.68	85.74
ER	100	94.84
CR	100	68.31

CR = corrosion rate; ER = electrical resistance; HCP = half-cell potential.

Table 8. It is shown that though there are little differences between the percent contributions of Taguchi and Factorial methods, Factorial method, due to its production of higher R-square values, can be more applicable and the results can be more accurate. It was also confirmed by the results of another study,[50] showing that Factorial method is better than Taguchi method since the mean square error is less and the parameter design of the Factorial method provides a simple, systematic and efficient methodology for optimization process.

4 | CONCLUSIONS

From this study, the following conclusions were drawn:

1. In the case of evaluation of RC corrosion, the results of HCP and ER tests cannot be reliable; thus, a more powerful method like electrochemical technique is necessary in order to obtain more reasonable and accurate results.
2. The experimental and statistical results mainly indicate that the use of 10% MS and a low content of AEA (up to 0.7%) appropriately improve the corrosion behavior of RC specimens.
3. The optimization results indicate that MS is a more pronounced factor than AEA due to its higher contribution in improving the corrosion behavior of RC.
4. Although small differences were observed between the optimization results of Taguchi and Factorial methods, Factorial method is more applicable in the field of corrosion evaluation of RC and yields more accurate findings as compared to the Taguchi method.

ORCID

Hamid Eskandari-Naddaf http://orcid.org/0000-0001-9156-6103

REFERENCES

1. Kakooei S, Akil HM, Dolati A, Rouhi J. The corrosion investigation of rebar embedded in the fibers reinforced concrete. Construct Build Mater. 2012;35:564–570.
2. Karagöl F, Yegin Y, Polat R, Benli A, Demirboğa R. The influence of lightweight aggregate, freezing–thawing procedure and air entraining agent on freezing–thawing damage. Struct Concr. 2018. https://doi.org/10.1002/suco.201700133
3. Ziaei-Nia A, Tadayonfar G-R, Eskandari-Naddaf H. Effect of air entraining admixture on concrete under temperature changes in freeze and thaw cycles. Mater Today. 2018;5(2):6208–6216.
4. Eskandari H, Nic AM, Ghanei A. Effect of air entraining admixture on corrosion of reinforced concrete. Proc Eng. 2016;150:2178–2184.
5. Choi P, Yeon JH, Yun K-K. Air-void structure, strength, and permeability of wet-mix shotcrete before and after shotcreting operation: The influences of silica fume and air-entraining agent. Cem Concr Compos. 2016;70:69–77.
6. Mehta, P.K., Concrete: Structure, properties and materials. 1986. Englewood Cliffs, NJ: Prentice-Hall, Incorporated.
7. Neville AM. Properties of concrete. Vol 687. 4th ed. London, UK: Pitman Publishing, 2011;p. 331.
8. Van den Heede P, Furniere J, De Belie N. Influence of air entraining agents on deicing salt scaling resistance and transport properties of high-volume fly ash concrete. Cem Concr Compos. 2013;37:293–303.
9. Keleştemur O, Demirel B. Corrosion behavior of reinforcing steel embedded in concrete produced with finely ground pumice and silica fume. Construct Build Mater. 2010;24(10):1898–1905.
10. Madani H, Bagheri A, Parhizkar T, Raisghasemi A. Chloride penetration and electrical resistivity of concretes containing nanosilica hydrosols with different specific surface areas. Cem Concr Compos. 2014;53:18–24.
11. Sengul O. Use of electrical resistivity as an indicator for durability. Construct Build Mater. 2014;73:434–441.
12. Kouril M, Prosek T, Scheffel B, Degres Y. Corrosion monitoring in archives by the electrical resistance technique. J Cult Herit. 2014;15(2):99–103.
13. Leelalerkiet V, Kyung JW, Ohtsu M, Yokota M. Analysis of half-cell potential measurement for corrosion of reinforced concrete. Construct Build Mater. 2004;18(3):155–162.
14. Yodsudjai W, Pattarakittam T. Factors influencing half-cell potential measurement and its relationship with corrosion level. Measurement. 2017;104:159–168.
15. Wang D, Zhou X, Fu B, Zhang L. Chloride ion penetration resistance of concrete containing fly ash and silica fume against combined freezing-thawing and chloride attack. Construct Build Mater. 2018;169:740–747.
16. Song H-W, Pack SW, Nam SH, Jang JC, Saraswathy V. Estimation of the permeability of silica fume cement concrete. Construct Build Mater. 2010;24(3):315–321.
17. Sobhani J, Najimi M. Electrochemical impedance behavior and transport properties of silica fume contained concrete. Construct Build Mater. 2013;47:910–918.
18. Eskandari-Naddaf H, Ziaei-Nia A. Simultaneous effect of nano and micro silica on corrosion behaviour of reinforcement in concrete containing cement strength grade of C-525. Proc Manufact. 2018;22:399–405.
19. Jung MS, Kim KB, Lee SA, Ann KY. Risk of chloride-induced corrosion of steel in SF concrete exposed to a chloride-bearing environment. Construct Build Mater. 2018;166:413–422.
20. Li L et al. Synergistic effects of micro-silica and nano-silica on strength and microstructure of mortar. Construct Build Mater. 2017;140:229–238.
21. Fathi M, Yousefipour A, Farokhy EH. Mechanical and physical properties of expanded polystyrene structural concretes containing micro-silica and Nano-silica. Construct Build Mater. 2017;136:590–597.

22. Arel HŞ, Shaikh FUA. Effects of silica fume fineness on mechanical properties of steel fiber reinforced lightweight concretes subjected to ambient and elevated temperatures exposure. Struct Concr. https://doi.org/10.1002/suco.201700281
23. Kim H, Nam I, Lee H. Enhanced effect of carbon nanotube on mechanical and electrical properties of cement composites by incorporation of silica fume. Compos Struct. 2014;107:60–69.
24. Bai S, Jiang L, Xu N, Jin M, Jiang S. Enhancement of mechanical and electrical properties of graphene/cement composite due to improved dispersion of graphene by addition of silica fume. Construct Build Mater. 2018;164: 433–441.
25. Ghaemi-Fard M, Eskandari-Naddaf H, Ebrahimi GR. Genetic prediction of cement mortar mechanical properties with different cement strength class after freezing and thawing cycles. Struct Concr. https://doi.org/10.1002/suco.201700196
26. Eskandari-Naddaf H, Kazemi R. ANN prediction of cement mortar compressive strength, influence of cement strength class. Construct Build Mater. 2017;138:1–11.
27. Mahdinia S, Eskandari-Naddaf H, Shadnia R. Effect of main factors on fracture mode of mortar, *a graphical study*. Civil Eng J. 2017;3(10):897–903.
28. Standard, A., C136/C136M-14, 2015. Standard test method for sieve analysis of fine and coarse aggregates, 2014. West Conshohocken, PA: ASTM international.
29. ASTM. 260Standard specification for air-entraining admixtures for concrete. West Conshohocken, PA: ASTM International, 2001.
30. ASTM. Standard test method for corrosion potentials of uncoated reinforcing steel in concrete. West Conshohocken, PA: ASTM International (cit. on pp. 53, 92, 95), 2015.
31. ASTM. Standard test method for bulk electrical conductivity of hardened concrete. West Conshohocken, PA: ASTM, 2012.
32. Clayton CR. Materials science and engineering: An introduction: By WD Callister Jr.; New York: John Wiley & Sons, 2011.
33. Ahmad S. Reinforcement corrosion in concrete structures, its monitoring and service life prediction—A review. Cem Concr Compos. 2003;25(4): 459–471.
34. Korouzhdeh T, Eskandari-Naddaf H, Gharouni-Nik M. An improved ant colony model for cost optimization of composite beams. Appl Artif Intell. 2017;31(1):44–63.
35. Robinson TJ, Borror CM, Myers RH. Robust parameter design: A review. Qual Reliab Eng Int. 2004;20(1):81–101.
36. Eskandari-Naddaf H, Azimi-Pour M. Performance evaluation of dry-pressed concrete curbs with variable cement grades by using Taguchi method. Ain Shams Eng J. 2016. https://doi.org/10.1016/j.asej.2016.09.004
37. Medan N et al. Taguchi versus full factorial design to determine the equation of impact forces produced by water jets used in sewer cleaning. MATEC web of conferences. EDP Sciences, 2017. https://doi.org/10.1051/matecconf/201711203007
38. Wang S, Huang G. A multi-level Taguchi-factorial two-stage stochastic programming approach for characterization of parameter uncertainties and their interactions: An application to water resources management. Eur J Oper Res. 2015;240(2):572–581.
39. Roy RK. A primer on the Taguchi method. Southfield, MI: Society of Manufacturing Engineers, 2010.
40. Pourbaix M. Atlas of electrochemical equilibria in aqueous solutions. Oxford, New York: NACA, 1984.
41. Astm C. Standard test method for half-cell potentials of uncoated reinforcing steel in concrete. Vol 4. ASTM Annual Book of ASTM Standards, West Conshohocken, PA: ASTM, 1991;p. 876–891.
42. Liu Z, Zhang Y, Jiang Q. Continuous tracking of the relationship between resistivity and pore structure of cement pastes. Construct Build Mater. 2014; 53:26–31.
43. Ghods P, Isgor O, Pour-Ghaz M. A practical method for calculating the corrosion rate of uniformly depassivated reinforcing bars in concrete. Mater Corros. 2007;58(4):265–272.
44. Rostami M, Behfarnia K. The effect of silica fume on durability of alkali activated slag concrete. Construct Build Mater. 2017;134:262–268.
45. Medeiros-Junior RA, Lima MG. Electrical resistivity of unsaturated concrete using different types of cement. Construct Build Mater. 2016;107:11–16.
46. Hussain SE. Corrosion resistance performance of fly ash blended cement concrete. Mater J. 1994;91(3):264–272.
47. Mendes JC, Moro TK, Figueiredo AS, et al. Mechanical, rheological and morphological analysis of cement-based composites with a new LAS-based air entraining agent. Construct Build Mater. 2017;145:648–661.
48. Corr DJ, Juenger MCG, Monteiro PJM, Bastacky J. Investigating entrained air voids and Portland cement hydration with low-temperature scanning electron microscopy. Cem Concr Compos. 2004;26(8):1007–1012.
49. Mukharjee BB, Barai SV. Assessment of the influence of Nano-silica on the behavior of mortar using factorial design of experiments. Construct Build Mater. 2014;68:416–425.
50. Rafidah A et al. *Comparison design of experiment (doe): Taguchi method and full factorial design in surface roughness*. Applied mechanics and materials. Switzerland: Trans Tech Publ, 2014.
51. Madadi A, Eskandari-Naddaf H, Gharouni-Nik M. Lightweight Ferrocement matrix compressive behavior: Experiments versus finite element analysis. Arab J Sci Eng. 2017;42(9):4001–4013.
52. Madadi A, Eskandari-Naddaf H, Shadnia R, Zhang L. Characterization of ferrocement slab panels containing lightweight expanded clay aggregate using digital image correlation technique. Construct Build Mater. 2018;180: 464–476.
53. Eskandari H, Madadi A. Investigation of ferrocement channels using experimental and finite element analysis. Eng Sci Technol. 2015;18(4):769–775.

AUTHOR BIOGRAPHIES

Anis Ghanei
Department of Civil Engineering, Hakim Sabzevari University, Sabzevar, Iran

Hamid Eskandari-Naddaf
Department of Civil Engineering, Hakim Sabzevari University, Sabzevar, Iran
hamidiisc@yahoo.com

Ali Davoodi
Materials and Metallurgical Engineering Department, Faculty of Engineering, Ferdowsi University of Mashhad, Iran

How to cite this article: Ghanei A, Eskandari-Naddaf H, Davoodi A. Corrosion behavior and optimization of air-entrained reinforced concrete, incorporating microsilica. *Structural Concrete*. 2018;1–9. https://doi.org/10.1002/suco.201800058